Biotribology 9 (2017) 18–23

Contents lists available at ScienceDirect

Biotribology

journal homepage: http://www.elsevier.com/locate/biotri

# Tunable Lubricin-mimetics for Boundary Lubrication of Cartilage

Kirk J. Samaroo [a], Mingchee Tan [b], Roberto C. Andresen Eguiluz [c], Delphine Gourdon [c,1], David Putnam [b,d], Lawrence J. Bonassar [a,b,*]

[a] Sibley School of Mechanical and Aerospace Engineering, Cornell University, Ithaca, NY, United States
[b] Meinig School of Biomedical Engineering, Cornell University, Ithaca, NY, United States
[c] Department of Materials Science and Engineering, Cornell University, Ithaca, NY, United States
[d] Smith School of Chemical and Biomolecular Engineering, Cornell University, Ithaca, NY, United States

ARTICLE INFO

*Article history:*
Received 3 July 2015
Received in revised form 1 February 2017
Accepted 7 February 2017
Available online 20 February 2017

*Keywords:*
Lubricin
Boundary lubrication
Cartilage
Osteoarthritis

ABSTRACT

The glycoprotein lubricin is the primary boundary lubricant of articular cartilage. Its boundary lubricating abilities arise from two key structural features: i) a dense mucin-like domain consisting of hydrophilic oligosaccharides and ii) an end terminus that anchors the molecule to articulating surfaces. When bound, lubricin molecules attract and trap water near a surface, reducing friction and facilitating glide. Synthetic analogues were previously created to mimic lubricin using thiol-terminated polyacrylic acid-*graft*-polyethylene glycol (pAA-*g*-PEG) brush copolymers. The PEG moiety was designed to mimic the mucin-like domain of lubricin and the thiol-terminus was designed to anchor the molecules to cartilage surfaces, mimicking the binding domain. In this study, these synthetic lubricin-mimetics were bound to gold-coated surfaces to characterize the relationship between the polymers' molecular architecture and their lubricating capacity. A library of nine copolymer brushes was synthesized using different sizes of pAA and PEG. Larger molecular weight polymers created smoother, more densely covered surfaces ($p < 0.05$). Additionally, the hydrodynamic sizes of the polymers in solution were correlated with their lubricating abilities ($p < 0.05$). Friction coefficients of cartilage against polymer-treated gold surfaces were lower than cartilage against untreated surfaces ($\Delta\mu_{eq} = -0.065 \pm 0.050$ to $-0.093 \pm 0.045$, $p < 0.05$).


## 1. Introduction

One of the primary functions of articular cartilage is to provide a low friction surface for diarthrodial joints. Lubrication of these joints depends on a variety of factors, most notably on synovial fluid and its constituents [1]. Lubricin, a mucinous glycoprotein found in synovial fluid and on the surface of articular cartilage [2], is an effective boundary lubricant. Lubricin reduces the boundary mode friction coefficient in cartilage-on-glass systems by as much as 70% [3]. Furthermore, the addition of lubricin and its derivatives to injured cartilage mitigates tissue degradation, slowing cartilage damage progression by up to 83% in some cases [4–7]. The restoration of frictional properties and amelioration of tissue damage demonstrates lubricin's significant therapeutic potential.

This potent lubricating ability arises from the structure of lubricin. The glycoprotein has a high molecular weight of 280 kDa, and is approximately 200 nm in length [8]. The central mucin domain consists of a core protein surrounded by a dense hydrophilic oligosaccharide brush [9]. Through the use of recombinantly produced termini, it was shown that the *C*-terminus of lubricin binds the protein to the cartilage surface, whereas the *N*-terminus controls aggregation [10]. It is believed that these structures work together to provide the lubricating mechanism of lubricin [11]. The *C*-terminus anchors and orients the protein at the cartilage surface, while the oligosaccharides of the mucin domain attract and retain water near the molecule. Collectively, these characteristics promote the formation of an aqueous film proximal to the cartilage surface, facilitating glide and reducing friction even under high normal loads or low velocities such as in boundary friction. However, lubricin is highly glycosylated with tandem repeating units, which makes its recombinant synthesis challenging and to date has limited its widespread use as a therapy for joint injury. While recent developments have addressed this challenge, its use is reported in only a small cohort of studies [12–15].

Because the proposed lubricating mechanism of lubricin depends solely on its structure, synthetic molecules made to mimic these attributes of lubricin demonstrated similar lubricating effects. We previously reported on synthetic polymer brushes with analogous structures to lubricin [16]. Like lubricin, the lubricin-mimetics were effective boundary lubricants of cartilage surfaces. A series of polyacrylic acid-*graft*-polyethylene glycol (pAA-*g*-PEG) lubricin-mimetics was synthesized (Fig. 1). Similar to lubricin, these polymers had two contributing

* Corresponding author at: Nancy E. and Peter C. Meinig School of Biomedical Engineering, 149 Weill Hall, Cornell University, Ithaca, NY 14853, United States.
*E-mail address:* lb244@cornell.edu (L.J. Bonassar).
[1] Current address: Department of Physics, University of Ottawa; Ottawa ON, K1N 6N5, Canada.

http://dx.doi.org/10.1016/j.biotri.2017.02.001
2352-5738/

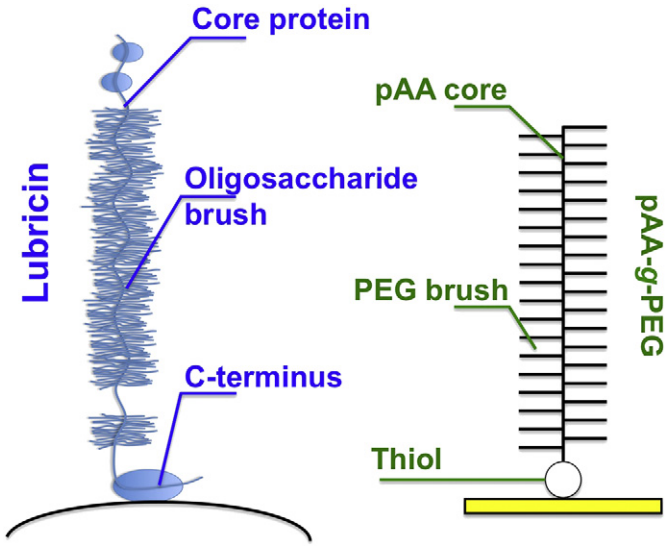


**Fig. 1.** Schematics of lubricin (left) and the pAA-*g*-PEG mimetic (right) are shown. Both configurations have a hydrophilic brush domain and an end terminus that anchors the molecules to surfaces.

features: a hydrophilic lubrication domain to maintain surface hydration and a binding terminus for attachment to the cartilage surface. This previous study noted clear dependence of lubrication on polymer composition, but the role of polymer structure and molecular conformation on lubricating function was not clear. Notably studying such phenomena is challenging, given that tissue roughness [17] is larger than the size of these polymers. A number of studies have utilized ideal surfaces to characterize lubricin [18–20] and other bio-inspired lubricants [21], but have not been used to analyze the current lubricant library.

The goal of this study was to gain a greater understanding of how the molecular architecture of lubricin-mimetics correlates to lubrication under boundary conditions. The specific objectives were to [1] describe and synthesize a series of synthetic lubricants that mimic the structure of lubricin [2]; examine the physical characteristics of these lubricants in solution and on idealized surfaces; and [3] determine the ability of the surface layers formed by these polymers to lubricate cartilage.

## 2. Materials and methods

### 2.1. Synthesis of lubricin-mimetics

According to the proposed lubrication mechanism, the moieties of lubricin most responsible for boundary lubrication are its *C*-terminus, which controls binding to surfaces, and its hydrophilic mucin domain, which attracts water. To mimic the brush-like mucin domain, hydrophilic polyethylene glycol (PEG) brushes were grafted to a polyacrylic acid (pAA) core. The pAA was synthesized via reversible addition–fragmentation chain-transfer (RAFT) polymerization using acrylic acid (AA), 4,4′-azobis 4-cyanopentanoic acid (A-CPA) and 4-cyanopentanoic acid dithiobenzoate (CPA-DB) under anhydrous, airtight and dark conditions [22]. The AA concentration was maintained at 3 mM while varying the concentrations of A-CPA and CPA-DB. A typical reaction scheme is as follows: AA (950 μl) was added to a flame dried 5 ml brown ampule with magnetic stirrer. Then CPA-DB (5.3 mg) was dissolved in nitrogen-purged methanol (2.9 ml) and added into the ampule containing AA. A-CPA (1.3 mg) was dissolved in 0.7 ml of nitrogen-purged methanol and added into the reaction ampule. Nitrogen gas was bubbled through the reaction mixture during and after the addition of each reagent for several minutes to prevent oxygen gas diffusion. Following the final nitrogen purge, the ampule was flame-sealed and placed in a 60 °C oil bath to initiate polymerization. After 48 h, the ampule neck was broken, and the reaction was exposed to air and cooled on ice to stop further reaction. The solution was then diluted and dialyzed against deionized water for 3 days and lyophilized to obtain a white, waxy powder.

The pAA-*graft*-PEG copolymer was synthesized via conjugation chemistry using 4-(4,6-dimethoxy-1,3,5-triazin-2-yl)-4-methyl morpholinium chloride (DMTMM) as the coupling agent based on a procedure developed previously [23]. An example reaction is as follows: pAA (10 mg, $M_W$ 107,600) and PEG-amine (0.151 g, $M_W$ 2000) were dissolved and mixed together in 2.4 ml of 0.1 M borate buffer (pH 8.5) in a 10 ml flask with stir bar. DMTMM (19.2 mg) dissolved in 0.6 ml of 0.1 M borate buffer was then added drop-wise to the mixture and pH was adjusted to 6–7 using 1 N HCl. The reaction was allowed to progress for 24 h and then dialyzed against deionized water for 3 days, before being lyophilized to recover a white powder.

### 2.2. Characterization and attachment of lubricin-mimetics

A series of copolymers with varied core and brush lengths was created to characterize their behavior both in solution and on surfaces. To characterize the behavior of the mimetics in solution, the hydrodynamic size of each polymer was measured via dynamic light scattering. pAA-*graft*-PEG copolymers were dissolved in filtered 1 M PBS at a concentration of 3 mg/ml, and hydrodynamic diameters were measured using a Malvern Zetasizer Nano ZS at 20 °C and a detector angle of 173 °C.

Next, the lubricating efficacy of the mimetics was assessed by anchoring them to gold substrates. Several studies have examined the formation of self-assembled monolayers through the use of thiol-gold interactions [24–26]. The thiol-terminus of the lubricin-mimetics bound to gold-coated glass slides, facilitating friction evaluation. Using a Varian Bell Jar Thermal Evaporator under a vacuum of approximately $10^{-7}$ Torr, a 10 nm-thick chromium layer and a subsequent 20 nm-thick layer of gold were deposited on polished glass slides. Each polymer was dissolved in deionized water (3 mg/ml) and incubated on the gold surfaces for at least 24 h. The surfaces were then rinsed with deionized water to remove any unbound polymers.

Four polymer architectures (pAA sizes of 60 and 105 kDa, PEG sizes of 2 and 10 kDa) were used to characterize the extent of surface modification by the lubricin-mimetics. These four mimetics were chosen for their distinct differences in brush characteristics to better elucidate distinct structure-function relationships.

### 2.3. Atomic force microscopy (AFM)

Gold-coated glass substrates functionalized with the different lubricin-mimetic polymers were imaged while hydrated on a commercial AFM (Agilent PicoPlus). Conical $SiO_2$ probes with nominal radius of curvature of 9 nm mounted on compliant ($k = 0.3$ N/m) levers (Burker) were used for contact mode imaging. Height channel image analysis was performed in Gwyddion (Czech Metrology Institute) to quantify roughness (Ra), mean globule size, and coverage area by shifting minimum image data value to zero, then leveled by mean plane subtraction, and finally corrected for horizontal scars. Mean globule size and coverage area were calculated after applying a mask (10% of max height). Peak-to-peak distances were obtained from processed images and further analyzed with a custom written script (Matlab, MathWorks).

### 2.4. Cartilage lubrication

Full thickness patellofemoral groove cartilage was removed from one to three day old bovine calves with a scalpel, and subsequently frozen and stored at −20 °C [3]. At the time of testing, the tissue was thawed in a water bath at 37 °C. A biopsy punch and a scalpel were used to create 6 mm diameter by 2 mm thick discs maintaining the articular surface. The discs were immersed in a 1.5 M NaCl solution for 30 min to remove native lubricin from the surface without affecting the collagen or proteoglycan structure [10,27]. Cartilage samples were then immersed in PBS for 60 min to restore osmotic equilibrium.

Cartilage discs and glass slides were loaded into a custom cartilage-on-glass tribometer described previously [10]. For these experiments, the cartilage was tested against gold-coated glass slides loaded into the tribometer. An initial compressive normal strain of 40% was induced onto each cartilage disc; 1 h was given to allow the cartilage to reach mechanical equilibrium under this compressive strain. The tribometer was then used to linearly oscillate the cartilage discs against the slide surfaces in a PBS solution at an entraining speed of 0.3 mm/s, conditions known to be well within boundary lubrication for this system [3]. The time-dependent normal and shear loads were measured, and the friction coefficient of each sample was calculated from the ratio of the shear to the normal loads, $\mu_{eq} = F_{shear} / F_{normal}$ (Supplemental Fig. 1). The change in friction coefficients compared to unlubricated controls, $\Delta\mu_{eq}$, was used to assess lubricant lubricity. The temporal patterns observed were similar to those seen previously for boundary lubrication of cartilage on glass [3,28].

Five slides of each polymer were prepared. Five control slides were also prepared with a gold film deposition, but without any polymer treatment. Each slide was only used for one friction test. A different cartilage disc was tested against each prepared slide.

### 2.5. Statistics

A two-way ANOVA was used to compare the effects of pAA size and PEG size on surface characteristics. The normality of the data distributions was confirmed with both Kolmogorov-Smirnov and Shapiro-Wilk tests ($p < 0.05$). Linear regressions were used to analyze relationships between the means of the hydrodynamic sizes, surface characteristics, and the lubricating abilities of the polymers.

## 3. Results

### 3.1. Synthesis

A library of lubricin-mimetics was created with a range of backbone sizes and brush sizes (Table 1). Sizes of the pAA backbones ranged from $M_W$ 60 to 145 kDa, while sizes of the PEG side chain ranged from $M_W$ 2 to 10 kDa. Varying both backbone and brush length provided a library of nine biomimetic lubricants.

By changing these two parameters, the contour length, diameter, and hydrodynamic size of the lubricants were controlled. Hydrodynamic sizes of the polymers increased with pAA and PEG length and ranged from 47 to 111 nm, compared to 173 nm for lubricin [2], and 62 nm for LUB:1 [2,4].

### 3.2. Surface coverage

To evaluate the effect of each of the structural parameters varied in this study ($M_W$ of pAA and PEG), four lubricin-mimetics were used. The mimetics varied in pAA size (105 kDa and 60 kDa) and PEG size (10 kDa and 2 kDa). Gold-coated slides treated with the four different mimetics were imaged via AFM. Polymers of different molecular architectures and sizes had unique surface coverage patterns. Quantification and characterization of the AFM images of the gold-coated surfaces was conducted by determining the average surface roughness ($R_a$), the mean globule sizes, the fraction of area covered by polymer globules, and the peak-to-peak distances between the globules (Fig. 2). Larger polymers resulted in greater and more complete surface coverage. The mean globule size and mean coverage area increased with pAA backbone size ($p < 0.05$). The effect of PEG size was less pronounced ($p = 0.16$). Mean globule sizes for the mimetic-treated slides ranged from 31.5 to 62.6 nm, and the mean coverage area of the polymers on the gold surfaces ranged from 5.2 to 37.8%. The peak-to-peak distance metric is a measure of the number density of the polymers or globules formed on a surface. The peak-to-peak distances between globules for the surface layers formed by the three larger polymers varied minimally, whereas the mean peak-to-peak distance for pAA(60)-*g*-PEG [2] was significantly lower ($p < 0.05$).

The hydrodynamic size of the different lubricin-mimetics is a metric of how the molecules behave in solution. To better understand the relationships between the behaviors of the mimetics in solution and at surfaces, their surface characteristics were compared to their hydrodynamic sizes (Fig. 3). Polymers of larger hydrodynamic size had larger globule sizes that covered more area, providing lower surface roughness ($p < 0.05$) despite having lower packing densities ($p < 0.05$). Polymers with larger hydrodynamic sizes formed thicker and more complete networks on surfaces, characteristics previously shown to provide better boundary lubrication.

**Table 1**
pAA-*g*-PEG configuration and size.

| pAA size (kDa) | PEG size (kDa) | Hydrodynamic size (nm) |
|---|---|---|
| 60 | 2 | 47 |
| 60 | 5 | 67 |
| 60 | 10 | 91 |
| 105 | 2 | 81 |
| 105 | 5 | 103 |
| 105 | 10 | 105 |
| 145 | 2 | 84 |
| 145 | 5 | 89 |
| 145 | 10 | 111 |
| | | |
| Lubricin core (kDa) | Brush size (kDa) | Hydrodynamic size (nm) |
| 120 [29] | 0.4–2.3 [6,30] | 173 [2] |

### 3.3. Lubrication

To better understand how the lubricating functionality of the polymers on surfaces relates to their behavior in solution, the experimental library was expanded to nine mimetics. Each of the nine lubricin-mimetics effectively lubricated articular cartilage. Equilibrium coefficients of friction of the cartilage plugs were significantly lower ($p < 0.05$) in the presence of biomimetic polymers compared to controls lubricated by PBS alone, with the change, $\Delta\mu_{eq}$, ranging from $-0.065 \pm 0.050$ to $-0.093 \pm 0.045$. Although no statistical relationship was found between the measured surface characteristics and the lubricating abilities of the mimetic-modified slides ($p = 0.21$–$0.43$), the lubricating ability correlated well with the mimetics' hydrodynamic size ($p < 0.01$), with larger polymers lubricating more effectively (Fig. 4). This further suggests that the lubricin-mimetics with larger hydrodynamic sizes promoted the formation of thicker lubricating aqueous films.

While the lubricin-mimetics significantly lowered friction coefficients, the previously measured [3] $\Delta\mu_{eq}$ of cartilage in the presence of native lubricin against an opposing glass surface, $-0.16 \pm 0.035$, was still lower than that of any of the biomimetic lubricants. The polymers also did not achieve the hydrodynamic size of lubricin (173 nm), with the largest being 111 nm. Additionally, the $\Delta\mu_{eq}$ of LUB:1 tested in a cartilage-on-glass system [4], $-0.060 \pm 0.010$, was comparable to that of lubricin-mimetics of similar hydrodynamic size. Larger polymers also lubricated more effectively than LUB:1, which has been shown to prevent the progression of cartilage damage. Looking to future work, the lubricin-mimetics with larger hydrodynamic sizes lubricated more effectively; therefore an increase in hydrodynamic size through a combination of an increase in pAA and/or PEG may lead to lubricin-mimetics with comparable hydrodynamic sizes and lubricating ability of lubricin.

## 4. Discussion

In this study, a family of biomimetic boundary lubricants was synthesized to mimic the brush-like structure of the natural glycoprotein lubricin. The behavior of these molecules in solution was characterized via dynamic light scattering. The hydrodynamic sizes of the brush-like

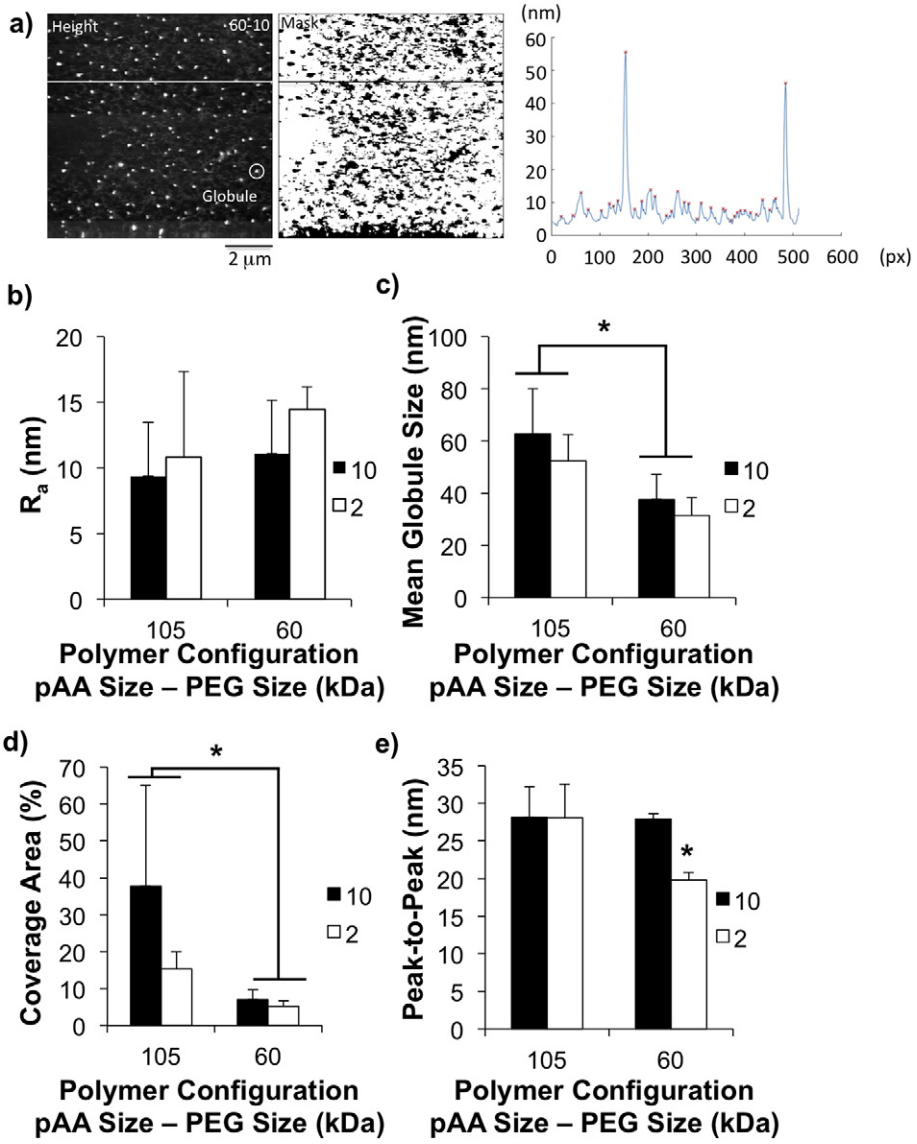


**Fig. 2.** a) AFM representative image indicating globule and one profile trace. The depositions of the polymer configurations on gold surfaces are characterized by b) surface roughness, c) mean globule size, d) coverage area, and e) peak-to-peak distances. No difference was seen in the surface roughness characteristics, whereas polymers with larger pAA size formed films with larger globules and more coverage ($p < 0.05$). Interestingly, the smallest polymer covered the least area, but still had the highest packing density (lowest peak-to-peak distances, $p < 0.05$). For each bar, sample sizes were $n = 5$ and error bars represent standard deviation.

pAA-*g*-PEG copolymers increased with pAA backbone length and PEG brush length. These lubricin-mimetics demonstrated significant lubricating ability when bound to gold and slid against articular cartilage. The equilibrium coefficient of friction, $\mu_{eq}$, was significantly lower in the presence of biomimetic polymers compared to unlubricated controls; $\Delta\mu_{eq}$ was as low as $-0.093 \pm 0.045$ ($p < 0.01$), lower than that for LUB:1 ($\Delta\mu_{eq} = -0.060 \pm 0.010$ in a cartilage-on-glass system). Using lubricin as a template, boundary lubricants that effectively lubricated articular cartilage were created.

The lubricin-mimetics were designed to modify the gold surfaces by creating a lubricating film, and the different mimetics resulted in surfaces with different characteristics. Specifically, the use of thiol-terminated polymers provided high affinity binding to gold-coated surfaces and enabled a direct assessment of the effect of molecular architecture on polymer spreading and lubrication. Polymers with larger pAA backbone sizes resulted in the formation of larger globules and denser coverage area. Larger polymers formed surfaces with more lubricant coverage to better promote the formation of lubricating films, facilitating movement, and lowering friction.

Additionally, clear correlations between the behavior of the mimetics in solution and on surfaces were observed. Polymers with larger hydrodynamic sizes formed smoother surfaces. This reinforces the idea that polymers that are larger in solution form smoother and more complete lubricating films on surfaces, and in turn enhance lubrication. Moreover, larger hydrodynamic sizes also suggest that the resultant film created on a surface would be thicker and allow for greater separation of articular surfaces, which also promotes the reduction of friction. Interestingly, the smallest polymers had better packing density but the lowest coverage area fractions. While these smaller lubricants pack more densely, they would form a thinner lubricating film and possibly a less complete network of lubricating brushes than their larger counterparts due to the discontinuity in total area covered. Interestingly, these smaller polymers lubricated best when bound to cartilage [16].

A correlation was observed where $\Delta\mu_{eq}$ decreased as the hydrodynamic size of the lubricant increased. While the $\Delta\mu_{eq} = -0.16 \pm 0.035$ for lubricin in a cartilage-on-glass system was lower than any of the synthetic lubricants tested, the hydrodynamic size of lubricin was also larger than any of the mimetic polymers synthesized. The observed

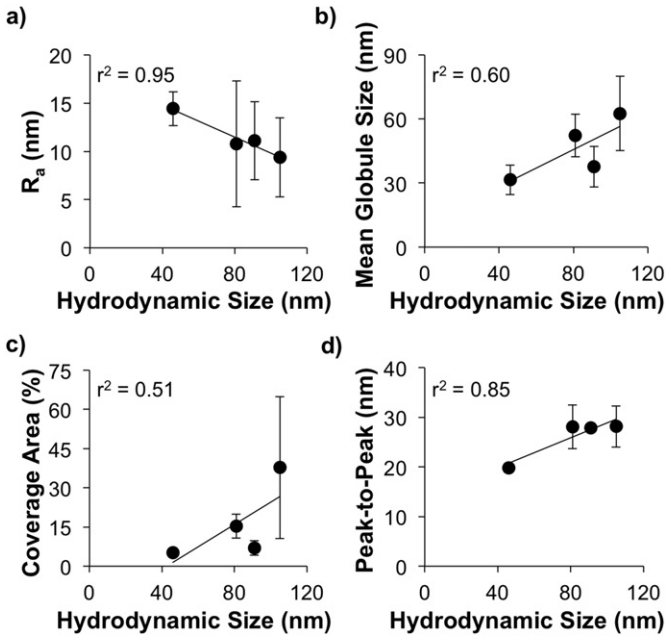


**Fig. 3.** The surface characteristics a) surface roughness, b) mean globule size, c) coverage area, and d) peak-to-peak distances are compared to the hydrodynamic sizes of the molecules, Polymer configurations of larger hydrodynamic size tended to form surfaces of lower surface roughness despite having lower packing densities. For each data point, sample sizes were n = 5 and error bars represent standard deviation.

trend suggests that biomimetic lubricants with large enough hydrodynamic sizes may lubricate as effectively as lubricin. Additionally, the larger polymers created smoother films allowing for better lubrication. This also reinforces the idea that larger lubricant hydrodynamic sizes correlate with thicker resultant lubricating films, and that thicker films have higher lubricity. This is consistent with other tribological studies examining boundary lubrication, including those investigating the use of PEGs to reduce friction coefficients on metal oxide and silicon oxide surfaces [31–33]. In these studies, poly(L-lysine)-*g*-PEG copolymers were used to create a boundary lubricating film. Increases in PEG length increased the fluid film thickness and lubricity. By modulating the structural parameters we were able to provide tunable, self-assembled aqueous lubrication analogous to the function of lubricin on cartilage.

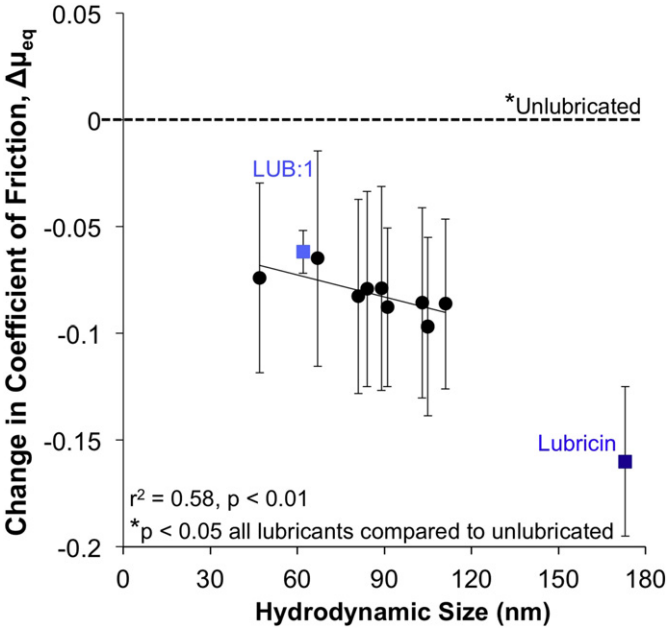


**Fig. 4.** The lubricin-mimetics effectively lubricated cartilage; the coefficients of all four polymers were significantly lower than that of the unlubricated case. Although none of the polymers approached the lubricating ability of lubricin in a cartilage-on-glass system [2,3], they were comparable to that of LUB:1 in a carilage-on-glass system [2,4]. An observed trend indicates that a polymer's lubricating ability increases with hydrodynamic size. Values obtained from the literature for lubricin and LUB:1 are consistent with this trend. Additionally, pAA-*g*-PEG brush polymers of similar hydrodynamic size to that of lubricin could potentially lubricate as effectively. For each data point, sample sizes were n = 5 and error bars represent standard deviation.

Furthermore, these results provide greater insight into the mechanism by which lubricin functions, confirming a connection between its structure and lubrication and supporting the proposed lubrication mechanism previously described [11]. The structure of the mucin domain is largely responsible for providing lubricin with its lubricating abilities. LUB:1 was previously shown to effectively lubricate cartilage despite having a mucin domain of approximately one-third the length of lubricin. The relative size and lubricating ability of LUB:1 was comparable to the lubricin-mimetics shown, emphasizing the dependence of lubricating ability on the structure of the lubricants. This lubricating ability is largely dependent on the hydrophilicity of the brush. The polymers with larger PEG side chains had larger hydrodynamic sizes, suggesting that more PEG will lead to enhanced lubrication. Lubricin exhibits similar behavior as its hydrophilic oligosaccharides are primarily responsible for its lubricating ability. Importantly, if the sugars are removed from the core protein, lubricin's lubricating efficacy drops by as much as 77% [9].

By mimicking the hydrophilic, brush-like structure of lubricin, pAA-*g*-PEG copolymers bound to gold surfaces were effective boundary lubricants of articular cartilage. Using different pAA backbone sizes and PEG side chain sizes, the lubricin-mimetics were tuned to create surfaces of different characteristics and different lubricating abilities. In this system, pAA-*g*-PEG polymers were bound to gold surfaces by self-assembly via a terminal thiol. In this system, polymer size in solution correlated with lubricating ability. Notably this relationship was not true when polymers were bound directly to cartilage [16], where some smaller polymers lubricated effectively. Collectively, these data point to the importance of understanding polymer lubricant conformation on both ideal surfaces and cartilage tissue.

Supplementary data to this article can be found online at http://dx.doi.org/10.1016/j.biotri.2017.02.001.

## Acknowledgments

This research was financially supported by the NIH/NIAMS under award 1 R01 AR066667-01 (to DP and LJB), the New York State Advanced Research Program (NYSTAR) (to LJB), the NSF under award DMR-1352299 (to DG) and DMR-05220404 Seed Grant (to LJB, DP and DG), the SAGE Fellowship (to KJS), the Provost's Diversity Fellowship (to KJS), the Morgan Fellowship (to MT), CONACYT under award 308671 (to RCAE), the use of core facilities through the Cornell Center for Materials Research award NSF DMR-1120296.

## References

[1] T.A. Schmidt, N.S. Gastelum, Q.T. Nguyen, B.L. Schumacher, R.L. Sah, Arthritis Rheum. 56 (2007) 882–891.
[2] D.A. Swann, F.H. Silver, H.S. Slayter, W. Stafford, E. Shore, Biochem. J. 225 (1985) 195–201.
[3] J.P. Gleghorn, A.R.C. Jones, C.R. Flannery, L.J. Bonassar, J. Orthop. Res. 27 (2009) 771–777.
[4] C.R. Flannery, R. Zollner, C. Corcoran, A.R. Jones, A. Root, M.A. Rivera-Bermúdez, T. Blanchet, J.P. Gleghorn, L.J. Bonassar, A.M. Bendele, E.A. Morris, S.S. Glasson, Arthritis Rheum. 60 (2009) 840–847.
[5] K.A. Elsaid, L. Zhang, K. Waller, J. Tofte, E. Teeple, B.C. Fleming, G.D. Jay, Osteoarthr. Cartil. 20 (2012) 940–948.
[6] E. Teeple, K.A. Elsaid, B.C. Fleming, G.D. Jay, K. Aslani, J.J. Crisco, A.P. Mechrefe, J. Orthop. Res. 26 (2008) 231–237.
[7] G.D. Jay, B.C. Fleming, B.A. Watkins, K.A. McHugh, S.C. Anderson, L.X. Zhang, E. Teeple, K.A. Waller, K.A. Elsaid, Arthritis Rheum. 62 (2010) 2382–2391.
[8] D.A. Swann, S. Sotman, M. Dixon, C. Brooks, Biochem. J. 161 (1977) 473–485.
[9] G.D. Jay, D.A. Harris, C.J. Cha, Glycoconj. J. 18 (2001) 807–815.

[10] A.R.C. Jones, J. Gleghorn, C.E. Hughes, L.J. Fitz, R. Zollner, S.D. Wainwright, B. Caterson, E.A. Morris, L.J. Bonassar, C.R. Flannery, J. Orthop. Res. 25 (2007) 283–292.
[11] J.M. Coles, D.P. Chang, S. Zauscher, Curr. Opin. Colloid Interface Sci. 15 (2010) 406–416.
[12] A. Al-Sharif, M. Jamal, L.X. Zhang, K. Larson, T.A. Schmidt, G.D. Jay, K.A. Elsaid, Arthritis Rheum. 67 (2015) 1503–1513.
[13] S. Abubacker, S.G. Dorosz, D. Ponjevic, G.D. Jay, J.R. Matyas, T.A. Schmidt, Ann. Biomed. Eng. 44 (2016) 1128–1137.
[14] M.L. Samsom, S. Morrison, N. Masala, B.D. Sullivan, D.A. Sullivan, H. Sheardown, T.A. Schmidt, Exp. Eye Res. 127 (2014) 14–19.
[15] K.A. Elsaid, L. Zhang, Z. Shaman, C. Patel, T.A. Schmidt, G.D. Jay, Osteoarthr. Cartil. 23 (2015) 114–121.
[16] K.J. Samaroo, M. Tan, D. Putnam, L.J. Bonassar, J. Orthop. Res. (2016)http://dx.doi.org/10.1002/jor.23370.
[17] E.D. Bonnevie, M.L. Delco, D. Galesso, C. Secchieri, L.A. Fortier, L.J. Bonassar, J. Biomech. (2017)http://dx.doi.org/10.1016/j.jbiomech.2016.12.034.
[18] B. Zappone, M. Ruths, G.W. Greene, G.D. Jay, J.N. Israelachvili, Biophys. J. 92 (2007) 1693–1708.
[19] B. Zappone, G.W. Greene, E. Oroudjev, G.D. Jay, J.N. Israelachvili, Langmuir 24 (2008) 1495–1508.
[20] S. Das, X. Banquy, B. Zappone, G.W. Greene, G.D. Jay, J.N. Israelachvili, Biomacromolecules 14 (2013) 1669–1677.
[21] A. Singh, M. Corvelli, S.A. Unterman, K.A. Wepasnick, P. Mcdonnell, J.H. Elisseeff, Nat. Mater. 13 (2014) 1–8.
[22] J.M. Pelet, D. Putnam, Macromolecules 42 (2009) 1494–1499.
[23] J.M. Pelet, D. Putnam, Bioconjug. Chem. 22 (2011) 329–337.
[24] K. Glinel, A.M. Jonas, T. Jouenne, J. Leprince, L. Galas, W.T.S. Huck, Bioconjug. Chem. 20 (2009) 71–77.
[25] A.W. Bridges, A.J. García, J. Diabetes Sci. Technol. 2 (2008) 984–994.
[26] S. Lee, Y.S. Shon, R. Colorado, R.L. Guenard, T.R. Lee, S.S. Perry, Langmuir 16 (2000) 2220–2224.
[27] E.D. Bonnevie, J.L. Puetzer, L.J. Bonassar, J. Biomech. 47 (2014) 2183–2188.
[28] J.P. Gleghorn, L.J. Bonassar, J. Biomech. 41 (2008) 1910–1918.
[29] G.D. Jay, D.E. Britt, C.J. Cha, J. Rheumatol. 27 (2000) 594–600.
[30] R.P. Estrella, J.M. Whitelock, N.H. Packer, N.G. Karlsson, Biochem. J. 429 (2010) 359–367.
[31] M.T. Müller, X. Yan, S. Lee, S.S. Perry, N.D. Spencer, Macromolecules 38 (2005) 5706–5713.
[32] S. Lee, M. Müller, M. Ratoi-Salagean, J. Vörös, S. Pasche, S.M. De Paul, H.A. Spikes, M. Textor, N.D. Spencer, Tribol. Lett. 15 (2003) 231–239.
[33] M. Müller, S. Lee, H.A. Spikes, N.D. Spencer, Tribol. Lett. 15 (2003) 395–405.